Testing randomness with photons by direct characterization of optical t-designs

Jonathan C. F. Matthews,[1,*] Rebecca Whittaker,[1] Jeremy L. O'Brien,[1] and Peter S. Turner[2,†]

[1]*Centre for Quantum Photonics, H. H. Wills Physics Laboratory and Department of Electrical and Electronic Engineering,*
University of Bristol, Merchant Venturers Building, Woodland Road, Bristol BS8 1UB, United Kingdom
[2]*Department of Physics, Graduate School of Science, University of Tokyo, 7-3-1 Hongo, Bunkyo-ku, Tokyo 113-0033, Japan*

Generating and characterizing randomness is fundamentally important in both classical and quantum information science. Here we report the experimental demonstration of ensembles of pseudorandom optical processes comprising what are known as t-designs. We show that in practical scenarios, certain finite ensembles of two-mode transformations—1- and 2-designs—are indistinguishable from truly random operations for 1- and 2-photon quantum interference, but they fail to mimic randomness for 2- and 3-photon cases, respectively. We make use of the fact that t-photon behavior is governed by degree-$2t$ polynomials (in the parameters of the optical process), to experimentally verify the ensembles' behavior for *complete* bases of polynomials, ensuring that average outputs will be uniform for arbitrary configurations. It is in this sense that a t-design is deemed to be a potentially useful pseudorandom resource.

PACS number(s): 42.50.Ex, 03.65.Wj, 05.40.−a, 42.50.St

Introduction. Randomness is a workhorse in science and technology, from simulating complex systems and modeling error to probabilistic computation and information security. In quantum mechanics, randomness is a fundamental feature, but additional (classical) randomness can be a powerful resource when purposely introduced into quantum protocols; examples include quantum communication [1], quantum algorithms [2], quantum data hiding [3], benchmarking unknown quantum processes [4–8], and verifying the boson sampling conjecture [9]. However, truly random quantum operations are inefficiently realizable both in principle and in practice. Here we report the realization and complete characterization of *pseudorandom* photonic quantum operator ensembles: so-called t-*designs* that simulate statistical properties of truly random operators using fewer resources [10,11]. We make use of the fact that t-photon behavior is governed by degree-$2t$ polynomials (in the optical process parameters), to perform complete experimental verification of the ensembles' behavior. We realize a 1-design and a 2-design, and show that 1- and 2-photon quantum interference [12,13] is sufficient for their complete verification. Furthermore, we show that 2- and 3-photon interference, respectively, can be used to test the limits of their pseudorandom properties. We apply these ideas to distinguish, with a fixed measurement setting, pseudorandom 1-design polarization rotations from Haar random unitaries in a situation where process tomography using single photon states would fail.

Unitary processes transform one pure quantum state to another. Realizing fair and unbiased random unitary operations requires sampling uniformly from a continuously infinite group. This group is equipped with a unique invariant (Haar) measure, which defines how one samples uniformly, without bias, over the whole set. However, "true" randomness is inefficiently realizable in practice, due to poor scaling of the number of random parameters with the size of the

system. Fortunately, sampling uniformly from a restricted subensemble of unitary operators can be done efficiently and still exhibits some of the desired statistical properties of truly random processes. Such pseudorandom operations are therefore sought after for applications in quantum protocols. Randomly sampled unitaries have been implemented experimentally, for example, in NMR [4,5], trapped ion [7], solid state [8], and photonic [14] qubits.

This notion of pseudorandomness is captured well by *unitary t-designs*. These are subensembles of quantum operations that, given t copies of a system, are statistically indistinguishable from a uniformly distributed superensemble. Equivalently, they are subensembles that have the same tth order moments as the uniform Haar ensemble, and thus they can be used to simulate statistical properties of truly random quantum operations with fewer resources. These statistical moments are given by polynomials in the parameters of the quantum operators in question (see below). The work presented here directly characterizes such pseudorandom operators experimentally.

Optical t-designs. Here we are concerned with the superensemble of all unitary polarization rotations of an optical channel. Ignoring global phase, these are parametrized by real variables $\{x_1, y_1, x_2, y_2\}$ with the constraint $x_1^2 + y_1^2 + x_2^2 + y_2^2 = 1$, and expressed as

$$U = \begin{pmatrix} x_1 + iy_1 & x_2 + iy_2 \\ -x_2 + iy_2 & x_1 - iy_1 \end{pmatrix}. \qquad (1)$$

Probability distributions that govern the outcomes of any multiphoton interference experiment are polynomials in these variables, whose degree is dictated by the number of photons. In general, t-photon interference is modeled by a degree-$2t$ polynomial in the matrix elements of the unitary process [17] [Fig. 1(a)]. For example, the transition probability of one photon from input 2 to output 2 is the degree-2 polynomial $|U_{2,2}|^2 = x_1^2 + y_1^2$ (note that this exactly agrees with how the intensity of classically modeled light is distributed as it passes through U). Degree-4 polynomials describe 2-photon nonclassical interference, including the probability to detect
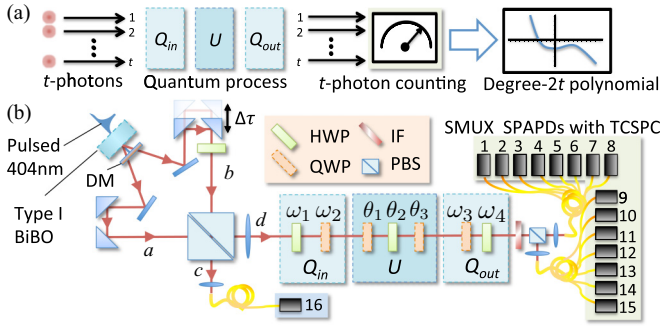
FIG. 1. (Color online) (a) t-photon interference is described by degree-$2t$ polynomials. (b) Our setup samples complete sets of independent degree-2 (degree-4) polynomials in the matrix elements of U using interference of 1-photon (2-photon) states, generated from spontaneous parametric down-conversion (SPDC) in type-1 BiBO. Polarized photon pairs generated in paths a and b are combined onto d in the photon-number state $|1\rangle_H |1\rangle_V$, using a half-wave plate (HWP) and a polarizing beam splitter (PBS). Degree-6 polynomials were sampled with the 3-photon state $|2\rangle_H |1\rangle_V$ in path d, observed by postselecting from the 4-photon term of pulsed SPDC state: 3-photons detected across single photon avalanche diodes (SPADs) 1–15 and one photon heralded at SPAPD 16 (see Supplemental Material for further details [15]). The quantum process $T = Q_{\text{out}} U Q_{\text{in}}$ was implemented using wave plates (QWP, HWP, dashed boxes). Photon-number-resolving detection [16] uses spatially multiplexed (SMUX) SPADs (1–15), used in conjunction with a commercial 16-channel time-correlated single photon counting system (TCSPC).

one photon in each output of U in a Hong-Ou-Mandel experiment [12], given by [13] $|U_{1,1}U_{2,2} + U_{1,2}U_{2,1}|^2$.

A unitary t-design [11] is defined in terms of such polynomials. Explicitly, a finite set $\mathfrak{D}_t$ containing K unitary operators, viewed as an ensemble with uniform distribution $1/K$, is defined to be a t-design if *every* degree-$2t$ polynomial [18] in the matrix elements of U, $f_{2t}(U)$, has the same average over $\mathfrak{D}_t$ as it does when averaged over the uniform ensemble of *all* unitaries:

$$\mathbb{E}_{\mathfrak{D}_t}[f_{2t}] = \sum_{U \in \mathfrak{D}_t} \frac{1}{K} f_{2t}(U)$$

$$= \int dU \, f_{2t}(U) = \mathbb{E}_{\text{Haar}}[f_{2t}]. \quad (2)$$

Uniformity in the continuous case is defined by the normalized unitary Haar measure dU, and there are methods for computing the integral over the unitary group (e.g., Ref. [19]). Note that a t-design is by definition also a $(t-1)$-design, hence experiments with t or fewer photons sampled over a t-design are statistically indistinguishable from the same experiments with operations sampled from the Haar distribution. Multiphoton interference, being governed by such polynomials, can therefore be used to verify the realization of a t-design, and $(>t)$-photon interference can also be used to test pseudorandomness as an alternative to standard process tomography.

The unitary operators we use to realize a 1-design are drawn from the uniformly distributed Pauli ensemble [20]

$$\mathfrak{D}_1 = \{I, iX, -iY, iZ\}. \quad (3)$$

Evidence that $\mathfrak{D}_1$ is a 1-design follows from the fact that single photons sequentially input into mode 1 will be distributed equally between output 1 (due to I and Z) and output 2 (due to X and Y), which agrees with the full Haar distributed random ensemble of SU(2) rotations: $\mathbb{E}_{\text{Haar}}[|U_{1,1}|^2] = \mathbb{E}_{\text{Haar}}[|U_{1,2}|^2] = 1/2$. A proof that $\mathfrak{D}_1$ is a 1-design can be obtained by showing the equality in Eq. (2) holds for each element of a complete basis of independent, degree-2 monomials in the real variables x_1, y_1, x_2, y_2; assuming unitarity there are nine, we choose:

$$f_2 \in \{x_1^2, x_1 x_2, x_2^2, x_1 y_1, x_1 y_2, x_2 y_1, x_2 y_2, y_1^2, y_1 y_2\}. \quad (4)$$

It is intuitive from a quantum optics perspective to see that $\mathfrak{D}_1$ is not a 2-design. Consider a Hong-Ou-Mandel experiment where we estimate the probability for two indistinguishable photons input into ports 1 and 2 to antibunch at the two outputs [12]. When U corresponds to a 50:50 beam splitter then there is ideally zero probability to detect one photon at each output. Therefore, when sampling over the entire Haar ensemble, the average probability for the photons to antibunch must be strictly less than 1. Averaging over $\mathfrak{D}_1$, however, will always yield an antibunching probability of exactly 1, hence Eq. (2) will not hold for all degree-4 polynomials.

The uniform ensemble of 12 operators listed in Table I is a 2-design, $\mathfrak{D}_2$. This is confirmed by showing Eq. (2) is satisfied with respect to the complete basis of (again, assuming unitarity) 25 degree-4 monomials:

$$f_4 \in \{x_1^4, x_1^3 x_2, x_1^2 x_2^2, x_1 x_2^3, x_2^4, x_1^3 y_1, x_1^2 x_2 y_1, x_1 x_2^2 y_1, x_2^3 y_1,$$
$$x_1^3 y_2, x_1^2 x_2 y_2, x_1 x_2^2 y_2, x_2^3 y_2, x_1^2 y_1^2, x_1 x_2 y_1^2, x_2^2 y_1^2, x_1^2 y_1 y_2,$$
$$x_1 x_2 y_1 y_2, x_2^2 y_1 y_2, x_1 y_1^3, x_1 y_1^2 y_2, x_2 y_1^3, x_2 y_1^2 y_2, y_1^4, y_1^3 y_2\}.$$
$$(5)$$

Experiment. We implement each element of $\mathfrak{D}_2$ (and $\mathfrak{D}_1$) using a combination of two quarter-wave plates and one half-wave plate, as shown in the box labeled U in Fig. 1(b), with the settings θ_i given in Table I.

To verify experimentally that an ensemble $\mathfrak{D}_t$ of unitaries is a t-design, we must have access to a complete basis of polynomials; this requires some added control over the optical transformation. We achieve this by adding the reconfigurable

TABLE I. The wave plate settings for θ_i in degrees, as labeled in Fig. 1(b), to realize the elements of $\mathfrak{D}_2 \supset \mathfrak{D}_1$. We adopt the convention that rotation angles are from the vertical.

$U \in \mathcal{D}_2$	θ_1	θ_2	θ_3
I	0	90	0
iX	0	−45	0
$-iY$	45	90	−45
iZ	−45	90	−45
$(I + iX - iY + iZ)/2$	0	90	−45
$(I + iX + iY + iZ)/2$	−45	90	0
$(I - iX - iY + iZ)/2$	45	90	0
$(I - iX + iY + iZ)/2$	0	90	45
$(I + iX - iY - iZ)/2$	45	−45	0
$(I + iX + iY - iZ)/2$	0	−45	45
$(I - iX - iY - iZ)/2$	0	45	−45
$(I - iX + iY - iZ)/2$	−45	45	0

TABLE II. Wave plate settings ω_i in degrees for Q_{in}, Q_{out}, as labeled in Fig. 1(b), for accessing polynomials p_i (1-photon experiments) and q_i (2-photon experiments).

p_i	ω_1	ω_2	ω_3	ω_4	p_i	ω_1	ω_2	ω_3	ω_4
p_1	0	0	0	0	p_6	0	22.5	0	22.5
p_2	0	0	0	22.5	p_7	0	22.5	22.5	0
p_3	0	0	0	45	p_8	0	45	0	0
p_4	0	0	22.5	0	p_9	0	45	0	22.5
p_5	0	22.5	0	0					

q_i	ω_1	ω_2	ω_3	ω_4	q_i	ω_1	ω_2	ω_3	ω_4
q_1	0	0	0	0	q_{14}	0	45	0	60
q_2	0	0	0	22.5	q_{15}	0	45	22.5	0
q_3	0	0	0	60	q_{16}	0	45	22.5	22.5
q_4	0	0	22.5	0	q_{17}	0	60	0	0
q_5	0	0	22.5	22.5	q_{18}	0	60	0	22.5
q_6	0	0	45	22.5	q_{19}	0	60	0	60
q_7	0	22.5	0	0	q_{20}	0	60	22.5	0
q_8	0	22.5	0	22.5	q_{21}	0	60	22.5	22.5
q_9	0	22.5	0	60	q_{22}	0	120	0	0
q_{10}	0	22.5	22.5	0	q_{23}	0	120	0	22.5
q_{11}	0	22.5	22.5	22.5	q_{24}	0	120	0	60
q_{12}	0	45	0	0	q_{25}	0	120	22.5	0
q_{13}	0	45	0	22.5					

polarization transformations $(Q_{\text{in}}, Q_{\text{out}})$, yielding the total unitary $T := Q_{\text{out}} U Q_{\text{in}}$, shown in Fig. 1. For each choice of configuration, the transition probability from a fixed input to a fixed output is a polynomial in the elements of U; thus we can now choose polynomials. The wave plate settings for $(Q_{\text{in}}, Q_{\text{out}})$ corresponding to our choice are given in Table II, labeled according to Fig. 1(b). We find these settings give complete bases of linearly independent [21] degree-2 and degree-4 polynomials as follows; nine 1-photon output probabilities corresponding to $|T_{1,1}|^2$, which we label $p_1, \ldots, p_9$ (e.g., $p_1 = x_1^2 + y_1^2$), and a set of twenty-five 2-photon probabilities $|T_{1,1}T_{2,2} + T_{1,2}T_{2,1}|^2$, which we label $q_1, \ldots, q_{25}$ (e.g., $q_1 = x_1^4 - 2x_1^2 x_2^2 + 2x_1^2 y_1^2 + x_2^4 - 2x_2^2 y_1^2 + y_1^4$). We then average each probability over $U \in \mathfrak{D}_t$, implemented as given in Table I, and thus arrive at an estimate for the left-hand side of Eq. (2) that we can use to verify uniformity.

Results. Figure 2 shows normalized 1-photon intensities $|T_{1,1}|^2$ extracted from the experiment, taken for $p_1, \ldots, p_9$ and averaged uniformly over the ensembles $\mathfrak{D}_1$ [Fig. 2(a)] and $\mathfrak{D}_2$
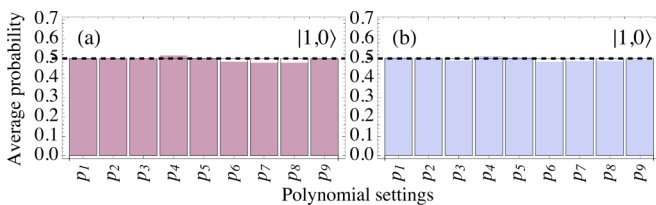

FIG. 2. (Color online) Polynomials $p_1, \ldots, p_9$ extracted from the measured normalized single photon intensity $|T_{1,1}|^2$, averaged over settings corresponding to (a) $\mathfrak{D}_1$ and (b) $\mathfrak{D}_2$. Measured distributions (solid color) are plotted with ideal theoretical values (empty boxes). Dashed lines represent the ideal Haar value $P_H = 1/2$, which is always uniform for normalized probability distributions.
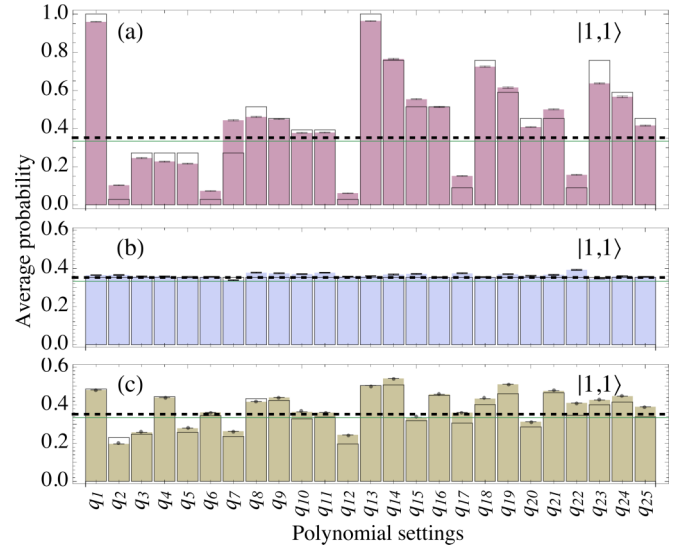

FIG. 3. (Color online) Polynomials $q_1, \ldots, q_{25}$ extracted from experiment by measuring the 2-photon correlation $|T_{1,1}T_{2,2} + T_{1,2}T_{2,1}|^2$ and averaging over settings that correspond to realizing (a) $\mathfrak{D}_1$, (b) $\mathfrak{D}_2$, and for comparison (c) 12 unitary operators chosen randomly from the Haar distribution that do not form a 2-design. Photon distinguishability alters the realized polynomials from their ideal values and the average they would converge to when sampling U over a Haar distribution (green line). This is characterized in the experiment and the ideal theoretical polynomials (empty boxes) and the Haar average (dashed line) are corrected accordingly (see Supplemental Material for details [15]). The average statistical fidelity, $\sum_i \sqrt{p_i q_i}$, between the probability distributions extracted from our experiment and the ideal distributions is $99.26 \pm 0.02\%$ for the 600 2-photon experiments used to generate these plots.

[Fig. 2(b)]. Both agree with the uniform Haar average over all unitaries. Since $p_1, \ldots, p_9$ are a complete basis, this agreement directly verifies the two ensembles $\mathfrak{D}_1$ and $\mathfrak{D}_2$ are both at least unitary 1-designs.

The difference in the behavior of $\mathfrak{D}_1$ and $\mathfrak{D}_2$ is clear when observing 2-photon interference. Figure 3 shows expected and measured 2-photon correlations $|T_{1,1}T_{2,2} + T_{1,2}T_{2,1}|^2$ taken for $q_1, \ldots, q_{25}$ and averaged uniformly over the ensembles $\mathfrak{D}_1$ [Fig. 3(a)] and $\mathfrak{D}_2$ [Fig. 3(b)]. The average of degree-4 polynomials over $\mathfrak{D}_1$ shows behavior clearly distinct from the uniform behavior that would be observed from averaging over the Haar measure (black dashed lines). Together with the results of Fig. 2(a), this agreement directly verifies the ensemble $\mathfrak{D}_1$ is a 1-design only. In contrast, the uniformity of the degree-4 polynomials averaged over $\mathfrak{D}_2$ [Fig. 2(b)] agrees closely with the average over the Haar measure. Since $q_1, \ldots, q_{25}$ is a complete set of degree-4 polynomials, this verifies the ensemble $\mathfrak{D}_2$ is at least a 2-design. For completeness, Fig. 3(c) shows 2-photon interference statistics averaged over a set of 12 matrices chosen from the Haar distribution [22]. The data illustrate that, in general, an ensemble of 12 operations—the size of $\mathfrak{D}_2$—is not sufficient to simulate the Haar average, though of course a larger ensemble eventually will (see Refs. [23,24] for convergence results). As t increases, it will be harder to distinguish between t- and $(t + 1)$-designs due to experimental noise.

TABLE III. Wave plate settings ω_i in degrees to access a selection of degree-6 polynomials using 3-photons.

p_i	ω_1	ω_2	ω_3	ω_4	p_i	ω_1	ω_2	ω_3	ω_4
r_1	94.0	117.3	64.9	24.5	r_4	179.7	11.36	24.6	108.1
r_2	129.5	67.1	118.3	6.8	r_5	1.9	114.0	162.5	160.7
r_3	112.8	67.9	159.2	3.6					

To complete the characterization of $\mathfrak{D}_2$, we use 3-photon interference for a set of five arbitrarily chosen degree-6 polynomial settings (labeled $r_1, \ldots, r_5$, with wave plate settings given in Table III). The data are shown in Fig. 4, verifying that $\mathfrak{D}_2$ is not a 3-design due to the existence of polynomials whose average over $\mathfrak{D}_2$ differs from the Haar value. Note that a single degree-6 polynomial that deviates from the Haar average is sufficient to demonstrate failure to simulate the Haar distribution.

Analysis of uniformity. How accurately the finite ensembles we realize mimic Haar distributed unitary matrices can be quantified by the uniformity of the average probabilities over the different polynomial settings, and how much they deviate from the expected Haar average in each case. We quantify the uniformity of the ensemble behavior in Fig. 5; note that while theory predicts that t-photon interference over a t-design should yield perfectly uniform results, experimental imperfections in realizing design elements can give rise to nonuniformity. Figure 5 indicates that variance, in particular, is an excellent discriminator for t-designs.

Example application. If a random optical channel is fluctuating slowly, then the ensemble could be broken down into its constituent elements and each interrogated by full process tomography [25], enabling x_1, y_1, x_2, y_2 to be reliably estimated and condition, Eq. (2), tested mathematically. When probing individual elements of an ensemble is limited, it may be convenient to use multiphoton states with a fixed measurement to directly distinguish an ensemble from the Haar ensemble. Figure 6 shows the real-time failure of a photonic 1-design to behave Haar randomly in the low photon rate regime. The wave plate configurations U were set to realize uniformly at random one of the four $\mathfrak{D}_1$ operations, and Q_{in} and Q_{out} were fixed to realize the polynomial q_{19}. For each implementation of U, we

FIG. 5. (Color online) Uniformity of each data set, plotted in terms of (a) the variance over the set of polynomials measured and (b) the maximum deviation of the average probability, as a percentage, from the expected Haar average (black dashed line in Fig. 2 and green solid lines in Figs. 3 and 4).

estimate the probability distribution of each 2-photon detection outcome using $O(10)$ correlated detection events, which yields a noisy estimate of the distribution that is insufficient to perform reliable process tomography; this could be performed with, on average, a single photon pair for each U by further attenuation. As we increase the number of samples of $\mathfrak{D}_1$ from 1 to 500, we compute a running average for the estimate of $P_{est} = |T_{1,1}T_{2,2} + T_{1,2}T_{2,1}|^2$ which converges to a value of 0.603 ± 0.001. For characterized photon indistinguishability, P_{est} should converge to 0.594 (blue line). Confidence that we are not sampling U according to the Haar measure is quantified by the number of standard deviations P_{est} is from $P_H = 1/3$—for example, for 11 trials (~ 220 photon pairs) is more than six standard deviations.

Conclusion. We have realized unitary 1- and 2-designs in two dimensions, using multiphoton interference for a complete verification of their pseudorandom properties. To
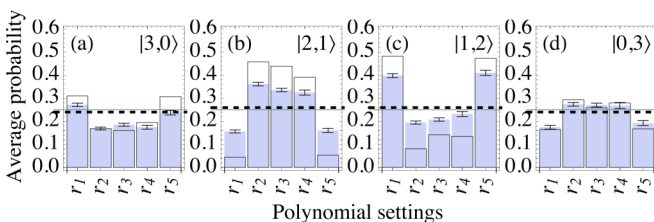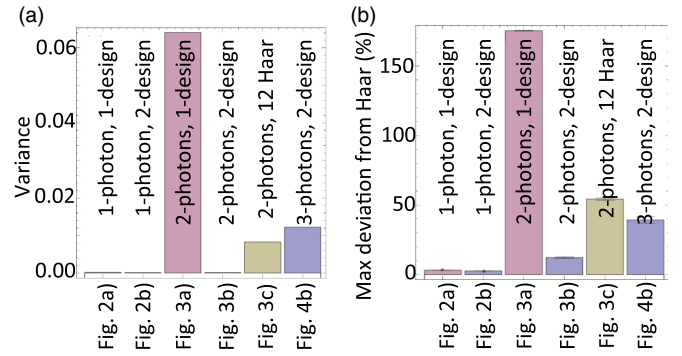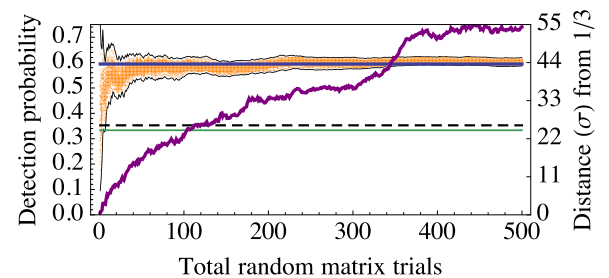

FIG. 4. (Color online) Detection outcomes for 3-photon polynomials r_i, averaged over $\mathfrak{D}_2$. Solid color represents measured data, empty boxes represent theory, and error bars are computed from assuming Poisson-distributed detection noise. Haar averages for perfect interference and characterized photon distinguishability are marked by the black dashed and green lines, respectively. The average statistical fidelity between measured probability distributions and theory is $97.55 \pm 0.03\%$ for the seventy-two 3-photon experiments.

FIG. 6. (Color online) Left-hand axis: Running average of $P_{est} = |T_{1,1}T_{2,2} + T_{1,2}T_{2,1}|^2$ estimated from each of 64 independent 2-photon experiments (overlaid orange points) as U implements uniformly at random elements of $\mathfrak{D}_1$ for polynomial q_{19}. The blue line marks the value that P_{set} should ideally converge to, taking into account characterized indistinguishability of photon pairs (see Supplemental Material [15]). Green and black dashed lines mark the values that P_{est} would converge to when sampling uniformly from the Haar measure, for perfect and characterized indistinguishability, respectively. Right-hand axis, purple line: The number of standard deviations that P_{est} differs from the Haar average $P_H = 1/3$, quantifying confidence of directly discriminating a non-Haar ensemble.

do so, we have made use of the fact that multiphoton transition probabilities are polynomials in the matrix elements of optical unitaries. In general, $(t+1)$-photon interference can be used to distinguish a t-design from a truly random ensemble of unitary operations. Although this can be mimicked with a reduced visibility of interference features using intensity correlation measurements of several input light fields [26], reaching the same visibility requires an overhead in measurement and data analysis [27,28]. Furthermore, we have demonstrated a scenario where standard process tomography would be incapable of inferring the "degree" of randomness (as given by a value of t). Interestingly, it has been suggested that such ensembles will likely be required to demonstrate conjectured extra-classical capabilities of linear quantum optics [29].

[1] A. Abeyesinghe, I. Devetak, P. Hayden, and A. Winter, Proc. R. Soc. London, Ser. A **465**, 2537 (2009).

[2] J. Radhakrishnan, M. Rötteler, and P. Sen, Algorithmica **55**, 490 (2009).

[3] P. Hayden, D. Leung, P. W. Shor, and A. Winter, Commun. Math. Phys. **250**, 371 (2004).

[4] J. Emerson, Y. S. Weinstein, M. Saraceno, S. Lloyd, and D. G. Cory, Science **302**, 2098 (2003).

[5] J. Emerson, M. Silva, O. Moussa, C. Ryan, M. Laforest, J. Baugh, D. G. Cory, and R. Laflamme, Science **317**, 1893 (2007).

[6] J. M. Epstein, A. W. Cross, E. Magesan, and J. M. Gambetta, Phys. Rev. A **89**, 062321 (2014).

[7] E. Knill, D. Leibfried, R. Reichle, J. Britton, R. B. Blakestad, J. D. Jost, C. Langer, R. Ozeri, S. Seidelin, and D. J. Wineland, Phys. Rev. A **77**, 012307 (2008).

[8] J. M. Chow, J. M. Gambetta, L. Tornberg, J. Koch, L. S. Bishop, A. A. Houck, B. R. Johnson, L. Frunzio, S. M. Girvin, and R. J. Schoelkopf, Phys. Rev. Lett. **102**, 090502 (2009).

[9] S. Aaronson and A. Arkhipov, in *Proceedings of the 43rd Annual ACM Symposium on Theory of Computing, San Jose* (ACM Press, New York, 2011), pp. 333–342.

[10] D. Gross, K. Audenaert, and J. Eisert, J. Math. Phys. **48**, 052104 (2007).

[11] C. Dankert, R. Cleve, J. Emerson, and E. Livine, Phys. Rev. A **80**, 012304 (2009).

[12] C. K. Hong, Z. Y. Ou, and L. Mandel, Phys. Rev. Lett. **59**, 2044 (1987).

[13] K. Mattle, M. Michler, H. Weinfurter, A. Zeilinger, and M. Zukowski, Appl. Phys. B **60**, S111 (1995).

[14] K. Banaszek, R. Demkowicz-Dobrzanski, M. Karpinski, P. Migdal, and C. Radzewicz, Opt. Commun. **283**, 713 (2010).

[15] See Supplemental Material at http://link.aps.org/supplemental/10.1103/PhysRevA.91.020301 for photon source details; mode-mismatch characterization; loss characterization and complete plots of multi-photon detection probabilities.

[16] D. Achilles, C. Silberhorn, C. Silwa, K. Banaszek, I. A. Walmsley, M. Fitch, B. C. Jacobs, T. B. Pittman, and J. D. Franson, J. Mod. Opt. **51**, 1499 (2004).

[17] Y. L. Lim and A. Beige, New J. Phys. **7**, 155 (2005).

[18] Elsewhere t-designs have been defined such that a distinction is made between the degrees of conjugate variables, but here we use only the real variables $\{x_1, y_1, x_2, y_2\}$.

[19] B. Collins and P. Sniady, Commun. Math. Phys. **264**, 773 (2006).

[20] The phases were chosen to give a representation of the unit quaternions $\mathbf{1} \leftrightarrow I$, $\mathbf{i} \leftrightarrow iX$, $\mathbf{j} \leftrightarrow -iY$, and $\mathbf{k} \leftrightarrow iZ$.

[21] Linear independence of the polynomials is confirmed by checking that the Gram matrix, defined here as the matrix of coefficients of a set of polynomials in the monomial basis, is full rank (9 for $t = 1$, 25 for $t = 2$).

[22] F. Mezzadri, Notices Amer. Math. Soc. **54**, 592 (2007).

[23] A. W. Harrow and R. A. Low, Commun. Math. Phys. **291**, 257 (2009).

[24] F. G. S. L. Brandao, A. W. Harrow, and M. Horodecki, arXiv:1208.0692.

[25] M. A. Nielsen and I. L. Chuang, *Quantum Computation and Quantum Information* (Cambridge University Press, Cambridge, 2000).

[26] Y. Bromberg, Y. Lahini, R. Morandotti, and Y. Silberberg, Phys. Rev. Lett. **102**, 253904 (2009).

[27] R. Keil, F. Dreisow, M. Heinrich, A. Tünnermann, S. Nolte, and A. Szameit, Phys. Rev. A **83**, 013808 (2011).

[28] Reference [27] uses three configurations to reconstruct the expansion of a two-photon quantum walk correlation function. Simulation of n-photon interference in this manner requires measurement and data analysis that grows with the $n!$ terms in the n-photon correlation function.

[29] C. Gogolin, M. Kliesch, L. Aolita, and J. Eisert, arXiv:1306.3995.